The impact of fluid-dynamic stress in stirred tank bioreactors on the synthesis of cellulases by Trichoderma reesei at the intracellular and extracellular levels

Tamiris Roque, Jérôme Delettre, Nicolas Hardy, Alvin W Nienow, Frédéric Augier, Fadhel Ben Chaabane, Catherine Béal

The impact of fluid-dynamic stress in stirred tank bioreactors on the synthesis of cellulases by *Trichoderma reesei* at the intracellular and extracellular levels

Tamiris Roque[1], Jérôme Delettre[2], Nicolas Hardy[1], Alvin W Nienow[3], Frédéric Augier[4], Fadhel Ben Chaabane[1], Catherine Béal[2]

1 IFP Energies Nouvelles, 1 et 4 avenue de Bois-Préau, 92852 Rueil-Malmaison, France;

2 AgroParisTech, UMR SayFood, 1 avenue Lucien Brétignières, 78850 Thiverval-Grignon, France;

3 School of Chemical Engineering, University of Birmingham, Edgbaston, Birmingham B15 2TT, United Kingdom;

4 IFP Energies Nouvelles, Rond-Point de l'Echangeur de Solaize, BP3, 69360 Solaize, France

**Corresponding author: frédéric.augier@ifpen.fr*

Abstract

Cellulases for bioethanol production are mainly made by fed-batch fermentation using a filamentous fungus, *Trichoderma reesei*. Agitation at different scales impacts on morphology, rheology and growth rate and can be correlated by $EDCF_{\varepsilon max}$. Typically, $EDCF_{\varepsilon max}$ is much smaller at commercial scale and fungal size, viscosity and growth rate are greater. Here, to increase understanding, continuous culture in 2.5 L bioreactors using two $EDCF_{\varepsilon max}$ values. The higher $EDCF_{\varepsilon max}$ decreased the cellulase production (concentration, 21 %; specific production rate, 24 %; protein yield, 20 %) whilst proteomic analysis showed, at an intracellular level, a decrease of cellulase and hemicellulase synthesis. An increase of stress proteins also occurred, which may help cells to limit the impact of fluid dynamic stress. Also, cellulase production during continuous culture at the bench varied with $EDCF_{\varepsilon max}$ similarly to that between bench and commercial scale during fed-batch culture.

Key-words: *Trichoderma reesei*; cellulases; fluid dynamic stress; scale-up/scale-down; proteomic analysis.

Highlights

- Higher values of $EDCF_{\varepsilon max}$ reduce production of extracellular cellulases
- This reduction is linked to a lowering of intracellular synthesis of cellulases
- Higher fluid dynamic stress leads to the appearance of stress proteins
- Intracellular stress proteins induce moderate changes in q_p from large ones in $EDCF_{\varepsilon max}$

1. Introduction

Second-generation (2G) bioethanol from lignocellulosic materials, is a good candidate to replace conventional fuels. Indeed, 2G bioethanol allows a reduction of about 85% of greenhouse gas emissions compared to fossil fuels (Morales et al., 2015). Also, 2G bioethanol uses lignocellulosic waste from the agri-food and forestry and does not compete with food. However, production costs remains high compared to ethanol from starch. This increase is mainly due to the high price of cellulases, the enzymes which hydrolyze lignocellulosic biomass into simple sugars. The 2G bioethanol price can be reduced if cellulases production costs are lowered (Hardy et al., 2017). Economy of scale is a way of doing so, requiring the use of bioreactors of several hundred cubic meters, a huge size compared with that at which the process is developed. With increasing scale, the medium in the bioreactor experiences increasing spatial heterogeneities (Amanullah et al., 2004; Lara et al., 2006) and the fluid dynamic stresses change (Hardy et al., 2017); and it is important to know what their impact will be.

Cellulolytic enzymes are mainly produced at industrial scale by the filamentous fungus *Trichoderma reesei* because of its high cellulases secretion capacity (Ferreira et al., 2014; Soni et al., 2018). As enzyme production is dissociated from growth, industrial cultures are often carried out in two steps: a batch phase for growth of the fungus followed by a fed-batch phase for the production of cellulases (Jourdier et al., 2013). During growth, *T. reesei* can use different carbon sources, but glucose is the most common (Hardy, 2016). As the *T. reesei* grows, it develops hyphae which form complex structures (Hardy et al., 2017b).. The complex morphology and high concentrations at the end of growth lead to a high viscosity medium with shear thinning behavior (Gabelle et al., 2012; Hardy et al., 2015; Quintanilla et al., 2015).

The production phase starts when the growth stops by limiting the carbon source to induce the production of cellulases (dos Santos Castro et al., 2014). In this phase, soluble sugars such as sophorose, cellobiose and lactose are used to induce the secretion of cellulases. In order to avoid further growth, an inductive substrate is fed continuously at an optimal limiting rate (Jourdier et al., 2013; Hardy et al., 2017). As *T. reesei* is a strictly aerobic microorganism, the dissolved oxygen concentration (dO_2) must be above the critical value, 15 % dO_2 (1.2 mg of O_2/L) (Marten et al., 1996) for the strain RUT-C30. However, the high viscosity at the end of the batch phase reduces mass transfer rates, and oxygen transfer (Albaek et al., 2012; Gabelle et al., 2012). To ensure dO_2 > 15 % dO_2 at this time, the power input has to be increased (Gabelle et al., 2012), enhancing the fluid dynamic stress on the mycelia.

There are many ways of characterizing fluid dynamic stress with changes in agitation intensity and with scale (Amanullah et al., 2004). Until the 1990s, the two most common were tip speed or specific power input, *P/V* (W.m^{-3}). However, in 1996, it was shown with the fungus, *P. chrysogenum*, that whilst tip speed increased with scale at constant specific power, damage to the organism was reduced (Jüsten et al., 1996). However, a new function which reduced with increasing scale, the energy dissipation/circulation function, *EDCF*, was able to correlate fungal breakage and various growth parameters, better than *P/V* (Jüsten et al., 1996). In essence, the *EDCF* concept is that fungus break to an equilibrium size dependent on the maximum specific energy dissipation rate, ε_{max} (W.m^{-3}) in a region close to the impeller and the frequency with which the organism passes through that region, $1/t_c$ (s) where the circulation time, $t_c = V/(Fl \cdot N \cdot D^3)$. Here, V (m^3) is the volume of broth in the bioreactor, N (rev.s^{-1}) the agitator speed, D (m) its diameter and Fl (dimensionless), its flow number. Because the circulation time increases with increasing scale even at constant

P/V, *EDCF* generally decreases with scale, sometimes markedly. There are a number of ways of assessing ε_{max} and a recently developed definition by Grenville et al. (2017) is $\varepsilon_{max} = 1.04 \,.\, x \,.\, \rho \,.\, Po^{\frac{3}{4}} \,.\, N^3 \,.\, D^2$. Here, *x* is the ratio of impeller diameter to trailing vortex diameter, a dimensionless characteristic of the impeller being used, as is *Po*, the power number; and ρ (kg. m^{-3}) is the density of the broth. In 2017, we used this definition of ε_{max} to develop (Hardy et al., 2017) an improved *EDCF* function, $EDCF_{\varepsilon max}$. We then used $EDCF_{\varepsilon max}$ to correlate the impact of the fluid dynamic stress associated with a variety of impellers on various process parameters during the initial batch growth phase of *T. reesei* fermentations at the bench scale and also with a multiple impeller combination at the industrial scale.

Other filamentous organisms to which the *EDCF* has been applied are *T. harzianum* (Rocha-Valadez et al., 2007), *A. oryzae* (Amanullah et al., 2002) and *P. ostreatus* (Fernández-Alejandre et al., 2016), where it was related to the transition of the organism from clumps to pellets. With *T. reesei* (Hardy et al., 2017), higher values of $EDCF_{\varepsilon max}$ reduced the mycelial size and specific growth rate (by up to 20 %) at the bench scale whilst at the commercial scale, as explained above, though the tip speed increased, $EDCF_{\varepsilon max}$ decreased leading to larger mycelia, higher viscosity and higher growth rates. However, as the bench runs were limited to the growth phase, cellulases were not produced; so the impact of fluid dynamic stresses on their production could not be investigated.

Previous work on the proteome of *T. reesei* has been studied in order to better identify the enzymes involved in lignocellulosic biomass degradation and the protein secretion profile under different environmental conditions (Herpoël-Gimbert et al., 2008). Apart from the common proteins involved in general metabolism, it mostly consists of two cellobiohydrolases (CBHI and CBH2), five endoglucanases (EGI, EGII, EGIII, EGIV and EGV)

and two β-glucosidases (BGLI and BGLII) that act in synergy to degrade lignocellulosic materials (Herpoël-Gimbert et al., 2008). Proteomic studies have investigated the secretome and/or intracellular proteins synthetized by filamentous fungi (Peterson and Nevalainen, 2012) by combining one-dimensional (1D) or two-dimensional (2D) gel electrophoresis with protein identification by liquid chromatography/ mass spectrometry. This technique allows the analysis of the multicomponent cocktail of cellulolytic enzymes secreted by *T. reesei* in culture media (Herpoël-Gimbert et al., 2008; Jun et al., 2013; Kubicek, 2013), and to investigate the differential protein synthesis at intracellular level (Bianco and Perrotta, 2015). The influence of carbon source (Jun et al., 2013; dos Santos Castro et al., 2014; Peciulyte et al., 2014), pH (Adav et al., 2011), light intensity (Stappler et al., 2017) and agitation intensity (Mukataka et al., 1988; Lejeune and Baron, 1995) on extracellular enzyme secretion has also been studied. However, except for Jun et al., 2013, which compared its intracellular proteome with various carbon sources; and Arvas et al., 2011 that studied the intracellular effects of growth rate and cell density in chemostat culture, the impact of culture conditions on intracellular protein synthesis by *T. reesei* remains poorly investigated. To our knowledge, the impact of fluid dynamic stress (here expressed as $EDCF_{\varepsilon max}$) on the synthesis of intracellular proteins by *T. reesei* has never been reported.

The objective of this work therefore was to characterize the effects of fluid dynamic stress on the production of both intracellular proteins and extracellular cellulases by *T. reesei*.

2. Material and Methods

2.1. Strain, preculture and culture media

The *T. reesei* strain used and the composition of the preculture medium and of the batch-culture medium were fully described previously (Hardy et al., 2017). For the production phase, the medium had the same composition as the batch-culture medium but it was supplemented with 0.83 $g.L^{-1}$ yeast extract instead of powdered corn steep liquor.

A 150 mL preculture was prepared in a 2 L Fernbach flask by mixing 135 mL of preculture medium and 15 mL of a sterile glucose solution at 250 $g\ L^{-1}$. The flasks were seeded with 1 mL of conidia to give a seeding rate of 10% and held in a shaker incubator (Multiron II, Infors, Bottmingen, Switzerland) for 72 hours at 30°C and 180 rpm with an orbit of 50 mm before being added into the bioreactor culture.

2.2. Bioreactor cultures using two different fluid dynamic stress conditions

This work is a follow on to that reported in Hardy et al. (2017). In that that study, the initial batch production of *T. reesei* was studied at the bench scale of 2.5 L working volume and at commercial scale. At the bench scale, a Rayneri centripetal turbine impeller (VMI-mixing, Montaigu, France) (see Fig 1) was used along with 3 others. All of the changes in process performance brought about by fluid dynamic stress for each impeller were successfully related to changes in $EDCF_{\varepsilon max}$. In order to move to continuous culture, a different bioreactor had to be selected and one of a similar size was available which used a Rayneri impeller. Since that impeller had fitted in well with the others in the earlier work, in order to have bench scale data in a similar sized bioreactor to aid comparison between the different aspects of the overall study, the present configuration was chosen.

157 A 3.0 L, dished bottomed, stirred bioreactor (ezControl BioBundle, Applikon Biotechnology,
158 Foster, CA, USA) with a working volume of 1.5 L, diameter T = 126 mm with a broth height,
159 H mm such that H/T = 1 and without baffles but with sufficient probes inserted to provide a
160 significant baffling effect. The Rayneri centripetal turbine impeller was 0.08 m diameter,
161 height, 0.045 m with Po = 2.0 and Fl = 1.3. The temperature was controlled at 27 °C, pH at
162 4.8 and dissolved oxygen concentration at 70 % by introducing a blend of air and nitrogen
163 (thereby altering the driving force for mass transfer) through a sparger. The total flow rate
164 was held constant at 0.8 L/min so that neither the dO_2 or flow rate changed during the
165 experiment (Hardy et al., 2017). However, as in earlier work (Herpoël-Gimbert et al., 2008),
166 to control to this dO_2 at the bench scale even with gas blending required a high P/V (Hardy
167 et al., 2017) of at least 6 kW. m^{-3}, which needed a minimum speed of 800 rpm. Such speeds
168 led to very high $EDCF_{\varepsilon max}$ compared to the commercial scale, where the circulation time is
169 significantly longer and the specific power was kept as low as possible for economic reasons.
170 Two complete runs, each consisting of 3 parts, were undertaken. In each, there was
171 an initial batch phase during which the fungus was grown at an agitation speed of 800 rpm
172 until a fungal biomass concentration of ~ 7.9 ± 0.2 $g.kg^{-1}$ was reached. Then, the continuous
173 phase of the run was begun, thereby commencing cellulase production. That time is marked
174 as 'start of continuous feed' on Fig 1 and from then, it was held at 800 rpm for another 150
175 hrs which allowed time for approximately 5 volume changes so that a steady state should
176 have been reached (Macauley-Patrick and Finn, 2008). The concentration of biomass and
177 the production of cellulases also indicated an approximate steady state for 50 hrs. At that
178 point, the speed was increased to 1700 rpm to give a higher fluid dynamic stress and then
179 kept constant with the same feed and discharge rate. This condition was held constant for
180 another approximately 140 hrs, equivalent to approximately 4 volume changes, sufficient to

approach another steady state and allow the impact of the change on biomass and intracellular and extracellular proteins to be assessed. The experiment was duplicated and samples were withdrawn at regular intervals for biomass and protein concentration measurements and those taken at the times noted on Fig 1 were used for proteomic analysis.

In the batch phase, the bioreactor contained 0.75 L 2N culture medium, 0.3 L water and 0.3 L glucose solution (150 $g.L^{-1}$) and it was inoculated with 0.15 L preculture to give an initial fungal concentration in the medium of 0.8 $g.kg^{-1}$. During the whole of the continuous phase, the constant feed and discharge rates of two solutions were lactose (180 $g.L^{-1}$) at 6 $mL.h^{-1}$ and the enriched 2N medium at 39 $mL.h^{-1}$ giving a dilution rate, D (0.03 h^{-1}) which since $D = \mu$, the growth rate, is also 0.03 h^{-1}.

2.3. Determination of concentrations in the culture medium

Biomass was quantified as described previously (Hardy et al., 2017) as was lactose following the method used for glucose. The concentration of the cellulases produced was quantified on filtered broth samples according to the Lowry method, by using the Protein Assay DC_{TM} kit (Biorad, Hercules, CA, USA) and a range of bovine serum albumin (BSA) concentrations from 0 to 1.5 $g.L^{-1}$ as standards (Hardy, 2016). β-glucosidase activity was measured as described by Jourdier et al. (2013). All analyses were performed in duplicate.

2.4. Proteomic analyses

The proteomic analyses of intracellular proteins were carried out in 3 steps: protein extraction, two-dimensional (2D) electrophoresis on sodium dodecyl sulfate polyacrylamide gel (SDS PAGE) and identification of proteins by mass spectrometry coupled to liquid chromatography.

The cytoplasmic proteins were first extracted by cell grinding from a biomass cake obtained by filtration as previously described. Initially, 0.2 g of biomass cake was washed and re-suspended as described previously (Wang et al., 2011). The cells were lysed with 0.6 g of glass beads (0.3 g of diameter 0.1 mm and 0.3 g of diameter 0.5 mm, Biospec Products, Bartlesville, OK, USA) in a FastPrep FP 120 equipment (Bio 101, Savant Instruments, Holbrook, AZ, USA), for four times with cycles of 30 s at an intensity of 6.5. After grinding the cells, the samples containing solubilized cytoplasmic proteins were centrifuged, purified with 60 U endonuclease (Biorad, Hercules, CA, USA) and precipitated, and their protein concentration was assayed using the colorimetric method of Bradford (1976) using bovine serum albumin as a standard in order to ensure 300 µg of proteins were present (Wang et al., 2011).

The separation of the extracted proteins was achieved by successive separation according to their isoelectric point by isoelectric focusing (IEF) and to their molecular weight by SDS-page electrophoresis. All samples from the two conditions were analyzed in triplicate from three different extractions. The cell extracts containing 300 µg of proteins were diluted in 350 µL of extraction buffer [31]. To perform IEF, the diluted samples were loaded onto Immobiline DryStrip gels (pI 4-7, 17 cm, Biorad) that were submitted to electric focusing at 20°C on an IEF Cell (Biorad, Hercules, CA, USA) to reach 73,000 Wh for about 24 hours.

After equilibration of the DryStrip gels, the second dimension separation was performed in SDS-polyacrylamide gels as described by Wang et al. (2011). Proteome image analysis was carried out with PDQuest 2-D software (Biorad) to compare the proteins density on the gels obtained from different conditions. Spots only present on one gel condition or showing a difference in density greater than a factor of 2 were considered as different between two conditions and retained for identification.

The spots corresponding to the differentially synthesized proteins were collected, washed separately with 50 mM ammonium hydrogen carbonate and 50 % acetonitrile and then dried. After digestion with 0.5 µg of trypsin (Promega, Madison, WI) and 50 mM ammonium hydrogen carbonate for 12 h at 37 °C, the supernatant containing peptides were used for protein identification by tandem mass spectrometry coupled to liquid chromatography (LC-MS / MS) using a LTQ-XL mass spectrophotometer (ThermoFinnigan, Waltham, MA, USA) (PAPPSO, Gif-sur-Yvette, France). The sequences were identified using the Joint Genome Institute databases (JGI, Walnut Creek, CA USA).

3. Results and Discussion

3.1. Estimation of the fluid dynamic stress, $EDCF_{\varepsilon max}$

In order to estimate ε_{max} (see Section 1), a value of x is required. The values (Grenville et al., 2017) for different impellers range from 12 to 17 but one is not available for the Rayneri impeller, which is a very different shape to others (see Fig 1). However, it produces radial flow as does a Rushton turbine which has an x value of 12 and this value is initially assumed here. Thus $EDCF_{\varepsilon max}$ was 1884 and 38,400 $kW.m^{-3}.s^{-1}$ respectively, a little higher than used previously (Hardy et al., 2017) because though similar speeds were used, here the bioreactor volume was smaller.

At the commercial scale, multiple impellers were used but the Rushton turbine provided most of the power input (Hardy et al., 2017). Thus, both the Po value and x of the Rushton turbine were chosen for the determination of $EDCF_{\varepsilon max}$ for the commercial scale, which as explained earller was very much lower at ~ 6.65 $kW.m^{-3}.s^{-1}$ (Hardy et al., 2017). Overall, $EDCF_{\varepsilon max}$ was the best correlator of hyphal size, broth rheology and growth rate for all the impellers and across these scales.

3.2. *Effect of fluid dynamic stress, $EDCF_{\varepsilon max}$, on the production of cellulases*

The details of the runs are given in Section 2.2. Figure 1 shows the biomass and protein concentration throughout the culture whilst Table 1 gives the mean biomass and cellulase concentrations at the first steady state (the lower $EDCF_{\varepsilon max}$) and the near-steady state at the higher $EDCF_{\varepsilon max}$. Table 1 also gives the value of a range of other process parameters obtained for these two conditions and p values from ANOVA tests for the results for the time periods indicated by the dotted lines on Fig 1. The variables describing the biomass (biomass concentration, specific growth rate, growth yield) were not influenced by the agitation rate (p-values higher than 0.05). The variables that characterize the protein production (protein concentration, specific production rate, production and conversion yields and β-glucosidase activity) were significantly affected by the $EDCF_{\varepsilon max}$ value (p-values lower than 0.05).

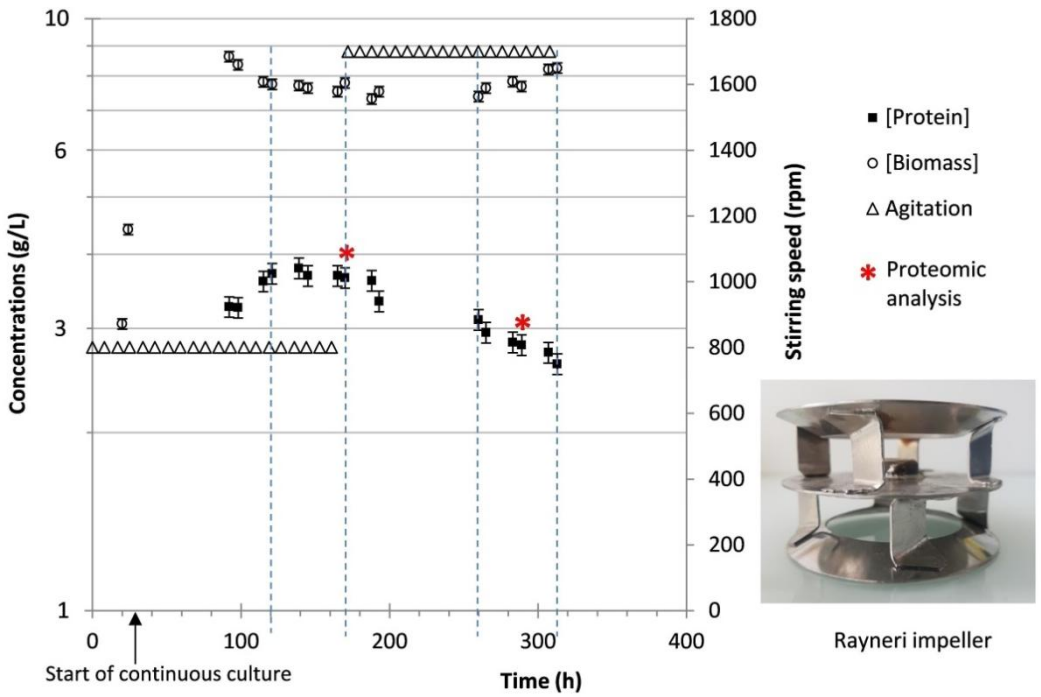

Figure 1: Biomass and protein concentrations during continuous culture agitated by a Rayneri centripetal turbine impeller (embedded image) at initially 800 rpm increasing to 1700 rpm ($EDCF_{\varepsilon max}$ 1884 and 38,400 $kW.m^{-3}.s^{-1}$ respectively). Dotted lines indicate time periods used for ANOVA tests. Error bars represent the standard deviation.

Table 1: Measured values of culture parameters and associated p-values at the two different speeds and $EDCF_{\varepsilon max}$ values

Stirring speed	800 rpm	1700 rpm	p-value
$EDCF_{\varepsilon max}$ (kW. m^{-3}. s^{-1})	1884	38400	na
Biomass concentration, X (g. kg^{-1})	7.7 ± 0.2	7.6 ± 0.2	0.538
Specific growth rate, μ (gX. gX^{-1}. h^{-1})	0.028 ± 0.01	0.028 ± 0.03	0.064
Protein concentration, P (g. kg^{-1})	3.7 ± 0.1	2.9 ± 0.1	0.001
Specific protein (cellulases)production rate, q_p (mg. gX^{-1}. h^{-1})	13.5 ± 0.5	10.3 ± 0.8	0.0002
Specific substrate consumption rate, q_s (mg. gX^{-1}. h^{-1})	0.084 ± 0.002	0.077 ± 0.002	0.0001
β-Glucosidase activity (IU/mL)	129.0 ± 1.7	107.9 ± 1.2	0.001
$Y_{X/S}$ (g. g^{-1})	0.35 ± 0.02	0.36 ± 0.04	0.471
$Y_{P/S}$ (g. g^{-1})	0.17 ± 0.01	0.13± 0.01	0.005
$Y_{P/X}$ (g. g^{-1})	0.48 ± 0.02	0.37 ± 0.02	0.002

The data presented corresponds to the mean values for each condition (800 and 1700 rpm) for the period shown on Figure 1 and their standard deviations. Legend as in Nomenclature ; na: not applicable.

The specific growth rate remained unchanged since a constant value was imposed by the constant dilution rate, *D*. However, constant biomass concentration is globally determined as cell dry weight. Ideally, the biomass concentration should also be subdivided into the percentage of active and inactive/damaged cells. However, reliable techniques for quantitatively measuring the viability of filamentous fungi are not available whether by fluorescent dyes, because of sampling issues, or by flow cytometry, because of the filamentous structure of the fungi which tends to block the capillaries. On the other hand, the constant biomass implies that it should all be active.

Table 1 and Figure 1 show that the specific production rate decreased by 24 % and the protein production yields in relation to sugar and to biomass concentration decreased by 20 % and 23 % respectively with p values again showing statistical significance. These results agree with previous studies on the effect of fluid dynamic stress on secondary metabolites production by filamentous fungus in stirred bioreactors. Jüsten et al. (1998) observed increase in *EDCF* with different impellers decreased penicillin production during fed-batch fermentations of *P. chrysogenum*. Lejeune and Baron (1995) and Mukataka et al.

289 (1988) found a lower production of cellulases at higher speeds with *T. reesei* cultures but did
290 not analyze the impact of different impellers or quantify hydrodynamic stress beyond
291 agitator speed. Reese and Ryu (1980) determined the effect of 'shear' on the stability of a
292 crude cellulase preparation of *T. reesei* and found that it caused deactivation of the enzyme
293 exoglucanase cellobiohydrolase (CBH), which slowed down cellulose digestion in a cellulosic
294 biomass hydrolysis. Ganesh et al. (2000) observed similar inactivation with increasing speed
295 in stirred reactors. These studies confirm that higher fluid dynamic stresses lead to a
296 decrease in cellulases production by *T. reesei* and to a deactivation of components of its
297 cellulolytic cocktail.

298 ***3.3. Effect of higher fluid dynamic stress on the synthesis of intracellular proteins***

299 Scanned pictures of the two SDS-PAGE gels from proteomic analysis of cells are given
300 in Figure 1 (Supplementary Material). The gels indicate intracellular proteins that were
301 differently synthesized at the two $EDCF_{\varepsilon max}$ values of 1884 and 38,400 $kW.m^{-3}.s^{-1}$
302 respectively. Image analysis of these gels allowed these proteins to be collected and
303 identified. In total, 30 spots, which corresponded to 24 different proteins, had their
304 synthesis modified as $EDCF_{\varepsilon max}$ increased. They were identified by tandem mass
305 spectrometry coupled with liquid chromatography (LC-MS/MS) and compared with *in silico*
306 data from sequence libraries as described in Section 2. At the higher $EDCF_{\varepsilon max}$, six proteins
307 were newly-synthesized (NW1 to NW6 in Table 2); six proteins were increasingly-
308 synthesized (up-regulated) by times 2 or more (UP1 to UP6, Table 3); and 18 proteins were
309 under-synthesized (down-regulated) by times 2 or more (UN1 to UN18, Table 4).

310 An analysis of Table 2 shows the increase in $EDCF_{\varepsilon max}$ only produced five new
311 proteins, as two of the 6 spots are isoforms of the same protein. Of the others, three assist

312 in protein quality control (including one chaperonin and two ubiquitin dependent
313 proteasomes) and are recognized as stress proteins. From Table 3, three up-synthesized
314 proteins are involved in the central carbon metabolism as they are related to
315 oxidoreductase activity (dihydrolipoyl dehydrogenase and FAD/NAD(P) domain-containing
316 protein) and Acetyl CoA biosynthesis (acetate kinase). The four others are involved in carbon
317 metabolism (adenosylhomocysteinase), proteolysis (glutamate carboxylpeptidase) and GDP-
318 mannose biosynthesis (phosphomannomutase). Finally, of the under-synthetized proteins
319 (Table 4), there are a number of isoforms and only 12 different ones are identified from 18
320 spots of which four relate to cellulolytic (glucosidases, endoglucanase and
321 cellobiohydrolases) and hemicellulolytic (xyloglucanases) activities. Of the eight others, one
322 involved putrescine biosynthesis (putative agmatine deiminase), two to transferase activity
323 (transketolase and uracil phosphoribosyl transferase) plus one isomerase (UDP-glucose-4-
324 epimerase), one kinase (diphosphomevalonate decarboxylase), one oxidoreductase
325 (NAD(P)H-dependent-D-xylose reductase), one involved in Ca^{2+} homeostasis (SGL domain-
326 containing protein) and one implicated in proteolysis (Zn-dependent exopeptidases).
327 Overall, two groups of proteins can be highlighted: under the higher $EDCF_{\varepsilon max}$, stress
328 proteins were over-synthesized (up-regulated) and cellulases were under-synthesized (down
329 –regulated).

330 **Table 2:** Proteins newly-synthesized by the increase from 800 to 1700 rpm ($EDCF_{\varepsilon max}$ 1884 and 38,400 $kW.m^{-3}.s^{-1}$ respectively)

Spot	Protein ID*	Protein description	*MW* (KDa) in the 2D gel	*IP* in the 2D gel	Coverage** (%)	Functional category
NW1	135423	Chaperonin HSP60	63.1	5.25	75	Chaperone molecular family
NW2	26797	20S proteasome subunit alpha type (homologs PSMA4 / PRE9)	26.2	6.12	73	Threonine endopeptidase activity - Ubiquitin-dependent protein
NW3	99350	20S proteasome alpha type (homologs PSMA6 / SCL1)	26.3	6.30	73	
NW4	80225	Uroporphyrinogen decarboxylase	39.2	5.99	71	Porphyrin biosynthesis
NW5 & NW6***	39524	Malate dehydrogenase	35.5 35.5	5.92 6.22	37 49	Oxidoreductase activity - Carbohydrate metabolism

331 *MW: molecular weight; IP: isoelectric pH; *Protein ID were obtained from JGI database; **Coverage corresponds to the percentage of the protein sequence*
332 *covered by identified peptides; ***Spots that correspond to isoforms of the same protein*
333

334

335 **Table 3:** Proteins over-synthesized from the increase from 800to 1700 rpm ($EDCF_{\varepsilon max}$ 1884 and 38,400 $kW.m^{-3}.s^{-1}$ respectively)

Spot	Protein ID*	Protein description	*MW* (KDa) in the 2D gel	*IP* in the 2D gel	Coverage** (%)	Log2 fold change	Functional category
UP1	78299	Dihydrolipoyl dehydrogenase	55.3	6.47	77	1.9	Oxidoreductase activity - Cell redox homeostasis
UP2	25190	FAD/NAD(P)-binding domain-containing protein	59.5	6.07	78	1.4	
UP3	97186	Phosphomannomutase	28.1	5.38	71	1.3	GDP-mannose biosynthetic process
UP4	137356	Glutamate carboxypeptidase	57.8	5.69	82	2.5	Proteolysis
UP5	99242	Acetate kinase	46.6	6.49	81	1.3	Acetyl-CoA biosynthesis
UP6	142425	Adenosylhomocysteinase	46.0	6.22	68	1.5	Nucleic acid and amino-acid metabolism

336 *MW: molecular weight; IP: isoelectric pH; *Protein ID were obtained from JGI database; **Coverage corresponds to the percentage of the protein sequence*
337 *covered by identified peptides*

338

339

Table 4: Proteins under-synthesized by the increase from 800 rpm to 1700 rpm ($EDCF_{\varepsilon max}$ 1884 and 38,400 kW.m^{-3}.s^{-1} respectively)

Spot	Protein ID*	Protein description	*MW* (KDa) in the 2D gel	*IP* in the 2D gel	Coverage** (%)	Log2 fold change	Functional category
UN1	122470	Exoglucanase II (1,4-β-cellobiohydrolase)	63.5	5.22	67	-2.3	Hydrolase activity – Cellulases
UN2	124438	Endo-β -1,4-glucanase	22.8	5.81	71	-2.3	
UN3 to UN7***	136547	β-D-glucoside glucohydrolase I	94.8 91.8 74.9 74.5 75.7	5.98 6.15 6.15 6.34 6.49	66 65 67 69 71	-1.5 -1.5 -2.8 -2.6 -2.8	
UN8 & UN9***	111943	Xyloglucanase	96.5 92.1	4.97 4.87	61 63	-2.4 -1.5	Hydrolase activity – Hemicellulase
UN10	108605	Uracil phosphoribosyl transferase	25.4	5.82	85	-1.2	Transferase activity - Nucleoside metabolism
UN11	111063	Peptide hydrolase	67.5	4.60	58	-2.3	Proteolysis
UN12 & UN13***	102903	Putative agmatine deiminase	47.0 46.8	4.55 4.65	84 40	-1.5 -2.6	Putrescine biosynthesis
UN14	99640	SMP30/gluconolactonase / LRE-like protein	33.7	5.12	75	-1.2	Ca^{2+} homeostasis and signal transduction
UN15	101957	Diphosphomevalonate decarboxylase	36.0	5.63	45	-1.1	Kinase activity - ATP binding - Phosphorylation
UN16	137982	UDP-glucose 4-epimerase	37.0	6.15	39	-1.3	Coenzyme binding - Isomerase activity - Cellular metabolism
UN17	94809	NAD(P)H-dependent D-xylose reductase	24.4	5.08	53	-1.6	Oxidoreductase activity
UN18	110941	Transketolase	74.7	6.39	72	-2.9	Transferase activity – Metal ion binding - Carbohydrate metabolism

*MW: molecular weight; IP: isoelectric pH; *Protein ID were obtained from JGI database; ** Coverage corresponds to the percentage of the protein sequence covered by identified peptides; ***Spots that correspond to isoforms of the same protein*

3.3.1. *Effect of higher fluid dynamic stress on the synthesis of stress proteins*

It is known that environmental stresses cause protein denaturation by aggregation and misfolding leading to loss of biological functions and cell apoptosis (Roller and Maddalo, 2013; Tiwari et al., 2015). Table 2 and Figure 1 (Supplementary Material) show the higher speed ($EDCF_{\varepsilon max}$) produces the chaperonin protein HSP60 and the ubiquitin-proteasome system which are known to reduce cell damage by acting on post-translational processes (Tiwari et al., 2015), correcting protein folding, helping refolding and stabilizing them under stress (Pickart, 1999). Specifically, HSP60 has a crucial role in synthesis, transportation, folding and degradation of proteins (Chen et al., 1999) and its over-expression under heat (Raggam et al., 2011; Tiwari et al., 2015) and heavy metal (Enjalbert et al., 2006) stress has been reported in fungal pathogens. Kashyap et al., 2016 observed its expression under saline stress in halotolerant fungus *P. clavariiformis*. The ubiquitin-proteasome system performs a similar function (Shang and Taylor, 2011; Kashyap et al. (2016) with various fungi; for example, nitrogen deprivation (Shang and Taylor, 2011), heat shock (Staszczak, 2008) and exposure to cadmium (Goller et al., 1998).

The present study clearly shows for the first time that the cells response to higher fluid dynamic stress is similar to that with other environmental stresses in order to protect themselves against irreversible damage.

3.3.2. *Effect of fluid dynamic stress on the synthesis of cellulases*

Figure 1 (Supplementary Material) and Table 4 show that at the higher $EDCF_{\varepsilon max}$, the synthesis of four intracellular cellulases decreased: glucosidases (β-D-glucoside glucohydrolase I), endoglucanases (endo-1,4-β-glucanases), cellobiohydrolases (exo-1,4-β-glucanases) and xyloglucanases. The first three make up the *T. reesei* cellulolytic cocktail

(Jourdier et al., 2013). Cellobiohydrolases attack the cellulose chains from the ends, releasing cellobiose molecules. Endoglucanases hydrolyze cellulose chains randomly, generate new ends accessible to cellobiohydrolases. β-glucosidase has the role of hydrolyzing into glucose the cellobiose released by the action of endoglucanases and cellobiohydrolases. This synergistic action is essential for hydrolysis of lignocellulosic biomass by the fungus (Kumar et al., 2008) as are xyloglucanases (Herpoël-Gimbert et al., 2008) for improving hydrolysis efficiency as the hemicellulolytic activity of this enzyme increases the surface area (Benkő et al., 2008).

The fact that the synthesis of cytoplasmic cellulases is negatively affected by higher fluid dynamic stress is strongly linked to the reduction of extracellular cellulases (Figure 1 and Table 1). This result indicates that the profile of extracellular proteins is directly linked to the synthesis of intracellular proteins, as demonstrated above from the proteomic analysis. This finding is original because, although some authors have reported the negative effects of 'shear' stress on the secretion of cellulases by *T. reesei* (Mukataka et al., 1988; Lejeune and Baron, 1995), the literature has not made any connection with the effect of fluid dynamic stress on the intracellular synthesis of cellulases.

3.4. Effect of scale on the production of cellulases

For this study in chemostat culture, $EDCF_{\varepsilon max}$ was 1884 $kW.m^{-3}.s^{-1}$ and 38400 $kW.m^{-3}.s^{-1}$ and the proteomic analysis showed that, as a result, a change took place at the intracellular level to protect the cells and partially maintain the production of cellulases. As a result of this protective action, though $EDCF_{\varepsilon max}$ increased substantially, the fall in cellulase production was relatively small, from 13.5 to 10.3 $g.kg^{-1}.\ h^{-1}$.

In the batch cultures previously reported (Hardy et al., 2017) (i.e. during the growth phase of the fermentation), $EDCF_{\varepsilon max}$ was a little smaller at the bench scale than here because a larger bench scale bioreactor was used. As usual, it was also much lower than here at the commercial scale (6.65 $kW.m^{-3}.s^{-1}$) for the reasons given earlier (Hardy et al., 2017) and in Section 3.1. The lower $EDCF_{\varepsilon max}$ was mirrored by increases in the growth rate, the viscosity of the broth and the size of the fungi.

At the commercial scale (Hardy et al., 2017), since the aim was to produce as much cellulase as possible, fed batch culture was used for the production phase to give a q_p of 17 $g.kg^{-1}h^{-1}$. In bench scale work (Hardy, 2016) related to this continuous culture study and the earlier batch study (Hardy et al., 2017), two fed batch cultures were also undertaken. These fed-batch studies were done in the same 3.5 L bioreactor (Hardy et al., 2017) with the Rayneri centripetal impeller at 1000 rpm to give an $EDCF_{\varepsilon max}$ of 2760 $kW.m^{-3}.s^{-1}$. The biomass concentration was controlled to 3.5 g/kg or 12 g/kg but the impact on the production of cellulases was not statistically significant (q_p = 11.9 ± 3.3 $g.kg^{-1}.h^{-1}$). Clearly, the scatter was large (Hardy, 2016). It is interesting to compare the small change in q_p for cellulase production with the very different $EDCF_{\varepsilon max}$ values in the continuous culture conditions reported here and those arising in fed-batch at the two very different scales. It is also convenient to assess whether the choice of x = 12 for the Rayneri impeller is an appropriate one.

Following the comparison of the various definitions of fluid dynamic stress in relation to process parameters in the initial batch production stage of *T. reesei* fermentation (Hardy et al., 2017), which showed the effectiveness of $EDCF_{\varepsilon max}$, a similar relationship

$$q_{p_{cont}} = A \cdot ln(EDCF_{\varepsilon max})_{cont} + B \qquad (1)$$

411 has been used to correlate the continuous culture results from the two $EDCF_{\varepsilon max}$ conditions.
412 Using the q_p value at the two $EDCF_{\varepsilon max}$ used, gives A = -1.05 and B = 21.4. If Eq (1 is now
413 applied to the fed-batch case at the bench (subscript fb1) and commercial scale (subscript
414 fb2) to give Eq (2,

$$q_{p_{fb2}} = q_{p_{fb1}} - A \cdot ln\left(EDCF_{\varepsilon max_{fb1}}/EDCF_{\varepsilon max_{fb2}}\right) \qquad (2)$$

415 where A = -1.05 and it is assumed that though different fermentation methods (batch, fed-
416 batch and continuous) give different product yields, the impact of fluid dynamic stress is the
417 same for the particular organism. Thus,

$$q_{p_{fb2}} = 11.9 + 1.05 \cdot ln(2760/6.65) = 18.3 \qquad (3)$$

418 This predicted value of q_p (18.3 $g.kg^{-1}h^{-1}$) at the commercial scale is impressively close to the
419 actual one (17 $g.kg^{-1}h^{-1}$) considering the large difference in the scales used for these two
420 fed-batch runs and that other factors can come into play at the commercial scale such as
421 increased levels of inhomogeneity due to the greater mixing time and pCO_2 and dO_2 due to
422 the static head.

423 The question regarding the impact of the value of *x* (the ratio of impeller diameter to
424 trailing vortex diameter) chosen for the Rayneri impeller can also be addressed in relation to
425 this type of analysis. Grenville et al. (2017) give a range of *x* values from 12 to 17 with 12
426 being the value for the Rushton turbine and chosen for the Rayneri because, though very
427 different from most impellers, they are both radial flow. If the other extreme, *x* = 17, is
428 chosen to test the range of possible impacts on this analysis, then the $EDCF_{\varepsilon max}$ values of the
429 continuous cultures reported in Table 1 are multiplied by 17/12, the *B* parameter of Eq.1
430 becomes 21.9 instead of 21.4, and the *A* parameter remains unchanged. Applying the same
431 *x* value of 17 for the bench scale fed batch run, $EDCF_{\varepsilon max}$ becomes 3910 $kW.m^{-3}.s^{-1}$. If this

value is used in Eq 3 then, since $EDCF_{\varepsilon max}$ for the large scale where the Rushton turbine dominates remains the same, the predicted value of q_p for the commercial scale becomes 18.6 $g.kg^{-1}.h^{-1}$. In this case, the choice of *x* clearly is not a significant factor in the analysis of the impact of fluid dynamic stress on the production of cellulases. Therefore given the similarity in flow pattern between the Rayneri impeller and the Rushton turbine, *x* = 12 remains the value of choice.

Overall, it can be concluded that not only can the use of the $EDCF_{\varepsilon max}$ function enable bench scale data to predict hyphal size, broth rheology and growth rate at the commercial scale (Hardy et al., 2017), it is also a powerful tool in aiding scale-up in relation to predicting the production of cellulases. Indeed, the production of cellulases at the commercial scale should not be compromised by fluid dynamic stresses. More importantly, the agitation intensity chosen should be based on ensuring it is sufficient to meet the demands of oxygen mass transfer and carbon dioxide stripping along with an adequate blending strategy, including sub-surface addition of nutrients and pH control chemicals (Amanullah et al., 2004). In addition, economic considerations must be taken into account.

4. Conclusion

T. reesei was cultivated in continuous cultures at two $EDCF_{\varepsilon max}$ values, the lower one (1884 $kW.m^{-3}.s^{-1}$) until a steady state was reached and the higher (38400 $kW.m^{-3}.s^{-1}$) until a near-steady state, sufficient to show a significant fall in protein production linked to measureable changes in intracellular proteins. This method of defining fluid dynamic stress has already been successful in correlating its impact in the batch growth phase of *T. Reesei* at the bench and commercial scale (Hardy et al., 2017). Here, the use of $EDCF_{\varepsilon max}$ provided a link between this bench scale continuous culture study with that batch work (Hardy et al.,

2017) and also related fed-batch culture to produce cellulases at the bench (Hardy, 2016) and commercial scale (~ 100 m^3) (Hardy et al., 2017). It is worthy of note, that a recent extensive review of scale-up methods concluded that the *EDCF* function was the best way of defining agitation intensity in bioprocessing (Böhm et al., 2019).

At the higher $EDCF_{\varepsilon max}$ at the bench scale, the concentration of the cellulases in the medium as well as the production yield and the specific production rate decreased by 21 %, 20 % and 24 % respectively. A proteomic analysis provided further insight that helped to explain these observations. Firstly, at the higher $EDCF_{\varepsilon max}$, the intracellular synthesis of all enzymes involved in cellulosic activity was decreased. On the other hand, stress proteins such as the HSP60 chaperone protein and the ubiquitin-proteasome system whose role is to protect the cells from the effects of fluid dynamic stress appeared. These findings demonstrate that at higher fluid dynamic stress, the fungus adapts itself by triggering protection and damage repair mechanisms at the intracellular level and by favoring its central metabolism to the detriment of other less essential functions, the combination of the two explaining the small decrease of cellulase biosynthesis even at much higher $EDCF_{\varepsilon max}$.

The higher extracellular cellulase production (q_p) at the lower $EDCF_{\varepsilon max}$ in continuous culture compared to that at the higher $EDCF_{\varepsilon max}$ is quantitatively similar to the increase in q_p during fed-batch fermentation at the commercial scale compared to that at the bench scale. Perhaps more importantly for the commercial aim of producing cellulases, the sensitivity to fluid dynamic stress is relatively small as the proteomic analysis explains.

Acknowledgements

The authors acknowledge the Plateforme d'Analyse Protéomique de Paris Sud Ouest (PAPPSO, Gif-sur-Yvette, France) for help in identifying the proteins. Funding: This work was supported by the Agence de l'Environnement et de la Maîtrise de l'Energie (ADEME, Angers, France) by providing financial support for the PhD study of Nicolas Hardy [number 2016SACLA017].

Nomenclature

D	dilution rate (h^{-1}) or impeller diameter (m)
dO_2	dissolved oxygen concentration (% of saturation value at ambient pressure)
$EDCF_{\varepsilon max}$	EDCF based on the maximum specific energy dissipation rate ($W.m^{-3}.s^{-1}$)
Fl	flow number of the impeller (dimensionless)
IP	isoelectric pH (dimensionless)
MW	molar weight (kDa)
N	rotation speed ($rev.s^{-1}$)
P	protein concentration ($g.kg^{-1}$) or power input from impeller (W)
Po	power number of the impeller (dimensionless)
q_p	specific protein production rate ($mgP.gX^{-1}.h^{-1}$)
q_s	specific substrate consumption rate ($mgS.gX^{-1}.h^{-1}$)
t	time (s in ε_{max} and $EDCF\varepsilon_{max}$ or h in Table 1)
t_c	circulation time (s^{-1})
V	volume of broth (L in Table 1 and m^3 in P/V)
x	ratio of impeller diameter to trailing vortex diameter
X	biomass concentration ($g.kg^{-1}$)
$Y_{X/S}$	biomass yield in relation to substrate ($g.g^{-1}$)
$Y_{P/S}$	protein yield in relation to substrate ($g.g^{-1}$)
$Y_{P/X}$	protein yield in relation to biomass ($g.\ g^{-1}$)
ε_{max}	maximum local specific energy dissipation rate ($W.m^{-3}$)
ρ	density ($kg.m^{-3}$)
μ	specific growth rate (h^{-1} or $gX.gX^{-1}.h^{-1}$)
Subscripts	
fb	fed-batch
cont	continuous culture

References

Adav, S.S., Ravindran, A., Chao, L.T., Tan, L., Singh, S., Sze, S.K., 2011. Proteomic analysis of pH and strains dependent protein secretion of *Trichoderma reesei*. J. Proteome Res. 10, 4579–4596. 10.1021/pr200416t.

Albaek, M.O., Gernaey, K.V., Hansen, M.S., Stocks, S.M., 2012. Evaluation of the energy efficiency of enzyme fermentation by mechanistic modeling. Biotechnol. Bioeng. 109 (4), 950–961. 10.1002/bit.24364.

Amanullah, A., Buckland, B., Nienow, A.W., 2004. Mixing in the fermentation and cell culture industries, in: Paul, E., Atiemo-Obeng, V., Kresta, S. (Eds.), Handbook of Industrial Mixing: Science and Practice. John Wiley & Sons, Inc., Hoboken N.J., pp. 1071–1170.

Amanullah, A., Christensen, L.H., Hansen, K., Nienow, A.W., Thomas, C.R., 2002. Dependence of morphology on agitation intensity in fed-batch cultures of *Aspergillus oryzae* and its implications for recombinant protein production. Biotechnol. Bioeng. 77 (7), 815–826.

Arvas, M., Pakula, T., Smit, B., Rautio, J., Koivistoinen, H., Jouhten, P., Lindfors, E., Wiebe, M., Penttilä, M., Saloheimo, M., 2011. Correlation of gene expression and protein production rate - a system wide study. BMC Genom. 12 (616), 1–25.

Benkő, Z., Siika-aho, M., Viikari, L., Réczey, K., 2008. Evaluation of the role of xyloglucanase in the enzymatic hydrolysis of lignocellulosic substrates. Enzyme Microb. Technol. 43, 109–114. 10.1016/j.enzmictec.2008.03.005.

Bianco, L., Perrotta, G., 2015. Methodologies and perspectives of proteomics applied to filamentous fungi: From sample preparation to secretome analysis. Int. J. Mol. Sci. 16, 5803–5829. 10.3390/ijms16035803.

Böhm, L., Hohl, L., Bliatsiou, C., Kraume, M., 2019. Multiphase stirred tank bioreactors – New geometrical concepts and scale-up approaches. Chem. Ing. Tech. 91 (12), 1724–1746. 10.1002/cite.201900165.

Bradford, M.M., 1976. A rapid and sensitive method for the quantitation of microgram quantities of protein utilizing the principle of protein-dye binding. Analytical Biochemestry 72, 248–254.

Chen, W., Syldath, U., Bellmann, K., Burkart, V., Kolb, H., 1999. Human 60-kDa heat-shock protein: A danger signal to the innate immune system. J. Immunol. Res. 162, 3212–3219.

dos Santos Castro, L., Pedersoli, W.R., Antoniêto, A. C. C., Steindorff, A.S., Silva-Rocha, R., Martinez-Rossi, N., Rossi, A., Brown, N.A., Goldman, G.H., Faça, V.M., Persinoti, G.F., Silva, R.N., 2014. Comparative metabolism of cellulose, sophorose and glucose in *Trichoderma reesei* using high-throughput genomic and proteomic analyses. Biotechnol. Biofuels 7 (41).

Enjalbert, B., Smith, D.A., Cornell, M.J., Alam, I., j, Nicholls, S., Brown, A.J.P., Quinn, J., 2006. Role of the Hog1 stress-activated protein kinase in the global transcriptional response to stress in the fungal pathogen *Candida albicans*. Mol. Biol. Cell. 17, 1018–1032.

Fernández-Alejandre, K.I., Flores, N., Tinoco-Valencia, R., Caro, M., Flores, C., Galindo, E., Serrano-Carreón, L., 2016. Diffusional and transcriptional mechanisms involved in laccases production by *Pleurotus ostreatus* CP50. Journal of biotechnology 223, 42–49. 10.1016/j.jbiotec.2016.02.029.

Ferreira, N.L., Margeot, A., Blanquet, S., Berrin, J.-G., 2014. Use of cellulases from *Trichoderma reesei* in the twenty-first century — Part I: Current industrial uses and future applications in the production of second ethanol generation, in: Gupta, V.K., Schmoll, M., Herrera-Estrella, A., Upadhyay, R.S., Druzhinina, I., Tuhoy, M.G. (Eds.), Biotechnology and Biology of *Trichoderma*. Elsevier, pp. 245–261.

Gabelle, J.-C., Jourdier, E., Licht, R.B., Ben Chaabane, F., Henaut, I., Morchain, J., Augier, F., 2012. Impact of rheology on the mass transfer coefficient during the growth phase of *Trichoderma reesei* in stirred bioreactors. Chem. Eng. Sci. 75, 408–417. 10.1016/j.ces.2012.03.053.

Ganesh, K., Joshi, J.B., Sawant, S.B., 2000. Cellulase deactivation in a stirred reactor. Biochem. Eng. J. 4, 137–141.

Goller, S.P., Gorfer, M., Kubicek, C.P., 1998. *Trichoderma reesei* prs12 encodes a stress and unfolded-protein-response-inducible regulatory subunit of the fungal 26S proteasome. Current Genetics 33, 284–290. 10.1007/s002940050338.

Grenville, R.K., Giacomelli, J.J., Padron, G., Brown, D.A.R., 2017. Mixing: Impeller performance in stirred tanks: Characterizing mixer impellers on the basis of power, flow, shear and efficiency. Chem. Eng. 124 (8), 42–51.

Hardy, N., 2016. Identification des critères d'extrapolation du procédé de production de cellulases par *Trichoderma reesei* en utilisant l'approche « scale-down ». Doctoral dissertation, France.

Hardy, N., Augier, F., Nienow, A.W., Béal, C., Ben Chaabane, F., 2017. Scale-up agitation criteria for *Trichoderma reesei* fermentation. Chem. Eng. Sci. 172, 158–168. 10.1016/j.ces.2017.06.034.

Hardy, N., Henaut, I., Augier, F., Béal, C., Ben Chaabane, F., 2015. Rhéologie des champignons filamenteux: Un outil pour la compréhension d'un procédé de production de biocatalyseurs utilisés pour la production de bioéthanol. Rhéologie 27, 43–48.

Herpoël-Gimbert, I., Margeot, A., Dolla, A., Jan, G., Mollé, D., Lignon, S., Mathis, H., Sigoillot, J.-C., Monot, F., Asther, M., 2008. Comparative secretome analyses of two *Trichoderma reesei* RUT-C30 and CL847 hypersecretory strains. Biotechnol. Biofuels 1 (18). 10.1186/1754-6834-1-18.

Jourdier, E., Cohen, C., Poughon, L., Larroche, C., Monot, F., Ben Chaabane, F., 2013. Cellulase activity mapping of *Trichoderma reesei* cultivated in sugar mixtures under fed-batch conditions. Biotechnol. Biofuels 6 (79). 10.1186/1754-6834-6-79.

Jun, H., Guangye, H., Daiwen, C., 2013. Insights into enzyme secretion by filamentous fungi: Comparative proteome analysis of *Trichoderma reesei* grown on different carbon sources. J. Proteom. 89, 191–201. 10.1016/j.jprot.2013.06.014.

Jüsten, P., Paul, G.C., Nienow, A.W., Thomas, C.R., 1996. Dependence of mycelial morphology on impeller type and agitation intensity. Biotechnol. Bioeng. 52, 672–684.

Jüsten, P., Paul, G.C., Nienow, A.W., Thomas, C.R., 1998. Dependence of *Penicillium chrysogenum* growth, morphology, vacuolation, and productivity in fed-batch fermentations on impeller type and agitation intensity. Biotechnol. Bioeng. 59 (6), 762–775.

Kashyap, P.L., Rai, A., Singh, R., Chakdar, H., Kumar, S., Srivastava, A.K., 2016. Deciphering the salinity adaptation mechanism in *Penicilliopsis clavariiformis* AP, a rare salt tolerant fungus from mangrove. J. Basic Microbiol. 56, 779–791. 10.1002/jobm.201500552.

Kubicek, C.P., 2013. Systems biological approaches towards understanding cellulase production by *Trichoderma reesei*. J. Biotechnol. 163, 133–142. 10.1016/j.jbiotec.2012.05.020.

Kumar, R., Singh, S., Singh, O.V., 2008. Bioconversion of lignocellulosic biomass: biochemical and molecular perspectives. Journal of Industrial Microbiology and Biotechnology 35, 377–391. 10.1007/s10295-008-0327-8.

Lara, A., Galindo, E., Ramírez, O., Palomares, L., 2006. Living with heterogeneities in bioreactors: Understanding the effects of environmental gradients on cells. Mol. Biol. 34, 355–382. 10.1385/MB:34:3:355.

Lejeune, R., Baron, G.V., 1995. Effect of agitation on growth and enzyme production of *Trichoderma reesei* in batch fermentation. Appl. Microbiol. Biotechnol. 43, 249–258.

575 Macauley-Patrick, S., Finn, B., 2008. Modes of Fermenter Operation, in: Mc Neil, B., Harvey, M.L.
576 (Eds.), Practical fermentation technology. John Wiley & Sons Ltd, Chichester,, pp. 69–95.
577 Marten, M., Velkvska, S., Khan, S., Ollis, D., 1996. Rheological, mass transfer, and mixing
578 characterization of cellulase-producing *Trichoderma reesei* suspensions. Biotechnol. Prog. 12 (5),
579 602–611.
580 Morales, M., Quintero, J., Conejeros, R., Aroca, G., 2015. Life cycle assessment of lignocellulosic
581 bioethanol: Environmental impacts and energy balance. Renew. Sustain. Energy Rev. 42, 1349–
582 1361. 10.1016/j.rser.2014.10.097.
583 Mukataka, S., Kobayashi, N., Sato, S., Takahashi, J., 1988. Variation in cellulase-constituting
584 components from *Trichoderma reesei* with agitation intensity. Biotechnol. Bioeng. 32, 760–763.
585 10.1002/bit.260320606.
586 Peciulyte, A., Anasontzis, G.E., Karlström, K., Larsson, P.T., Olsson, L., 2014. Morphology and enzyme
587 production of *Trichoderma reesei* Rut C-30 are affected by the physical and structural
588 characteristics of cellulosic substrates. Fungal Genetics and Biology 72, 64–72.
589 10.1016/j.fgb.2014.07.011.
590 Peterson, R., Nevalainen, H., 2012. *Trichoderma reesei* RUT-C30 – thirty years of strain improvement.
591 Microbiology 158, 58–68. 10.1099/mic.0.054031-0.
592 Pickart, C.M., 1999. Ubiquitin and the stress response, in: Latchman, D.S. (Ed.), Stress Proteins:
593 Handbook of Experimental Pharmacology. Springer-Verlag, Berlin, Heidelberg, 133–152.
594 Quintanilla, D., Hagemann, T., Hansen, K., Gernaey, K.V., 2015. Fungal morphology in industrial
595 enzyme production- Modelling and monitoring. Advances in biochemical
596 engineering/biotechnology 149, 29–54. 10.1007/10_2015_309.
597 Raggam, R.B., Salzer, H.J.F., Marth, E., Heiling, B., Paulitsch, A.H., Buzina, W., 2011. Molecular
598 detection and characterisation of fungal heat shock protein 60. Mycoses 54, 394-399.
599 10.1111/j.1439-0507.2010.01933.x.
600 Reese, E.T., Ryu, D.Y., 1980. Shear inactivation of cellulase of *Trichoderma reesei*. Enzyme Microb.
601 Technol. 2, 239–240.
602 Rocha-Valadez, J., Galindo, E., Serrano-Carreón, L., 2007. The influence of circulation frequency on
603 fungal morphology: dissipation rate cultures of *Trichoderma harzianum*. J. Biotechnol. 130 (4),
604 394–401. 10.1016/j.jbiotec.2007.05.001.
605 Roller, C., Maddalo, D., 2013. The molecular chaperone GRP78/BiP in the development of
606 chemoresistance: mechanism and possible treatment. Front. Pharmacol. 4, e00010, 1–5.
607 10.3389/fphar.2013.00010.
608 Shang, F., Taylor, A., 2011. Ubiquitin-proteasome pathway and cellular responses to oxidative stress.
609 Free Radic. Biol. Med. 51, 5–16. 10.1016/j.freeradbiomed.2011.03.031.
610 Soni, S.K., Sharma, A., Soni, R., 2018. Cellulases: Role in lignocelullosic biomass utilization, in: Lübeck,
611 M. (Ed.), Cellulases. Humana Press, New York, NY.
612 Stappler, E., Walton, J.D., Beier, S., Schmoll, M.a., 2017. Abundance of secreted proteins of
613 *Trichoderma reesei* is regulated by light of different intensities. Front. Microbiol. 8, e02586, 1–
614 14. 10.3389/fmicb.2017.02586.
615 Staszczak, M., 2008. The role of the ubiquitin-proteasome system in the response of the ligninolytic
616 fungus *Trametes versicolor* to nitrogen deprivation. Fungal Genetics and Biology 45, 328–337.
617 10.1016/j.fgb.2007.10.017.
618 Tiwari, S., Thakur, R., Shankar, J., 2015. Role of heat-shock proteins in cellular function and in the
619 biology of fungi. Biotechnol. Res. Int., 1–11. 10.1155/2015/132635.

620 Wang, Y., Delettre, J., Corrieu, G., Béal, C., 2011. Starvation induces physiological changes that act on
621 the cryotolerance of *Lactobacillus acidophilus* RD758. Biotechnol. Prog. 27 (2), 342–350.
622 10.1002/btpr.566.
623

Supplementary material

Figure 1 : Proteomic analysis of *T. reesei* cells: A) 800 rpm ($EDCF_{\varepsilon max}$ 1884 $kW.m^{-3}.s^{-1}$); B) 1700 rpm ($EDCF_{\varepsilon max}$ 38400 $kW.m^{-3}.s^{-1}$); UN1-UN19: under-synthesized proteins; UP1-UP7: over-synthesized proteins; NW1-NW6: newly-synthesized proteins.

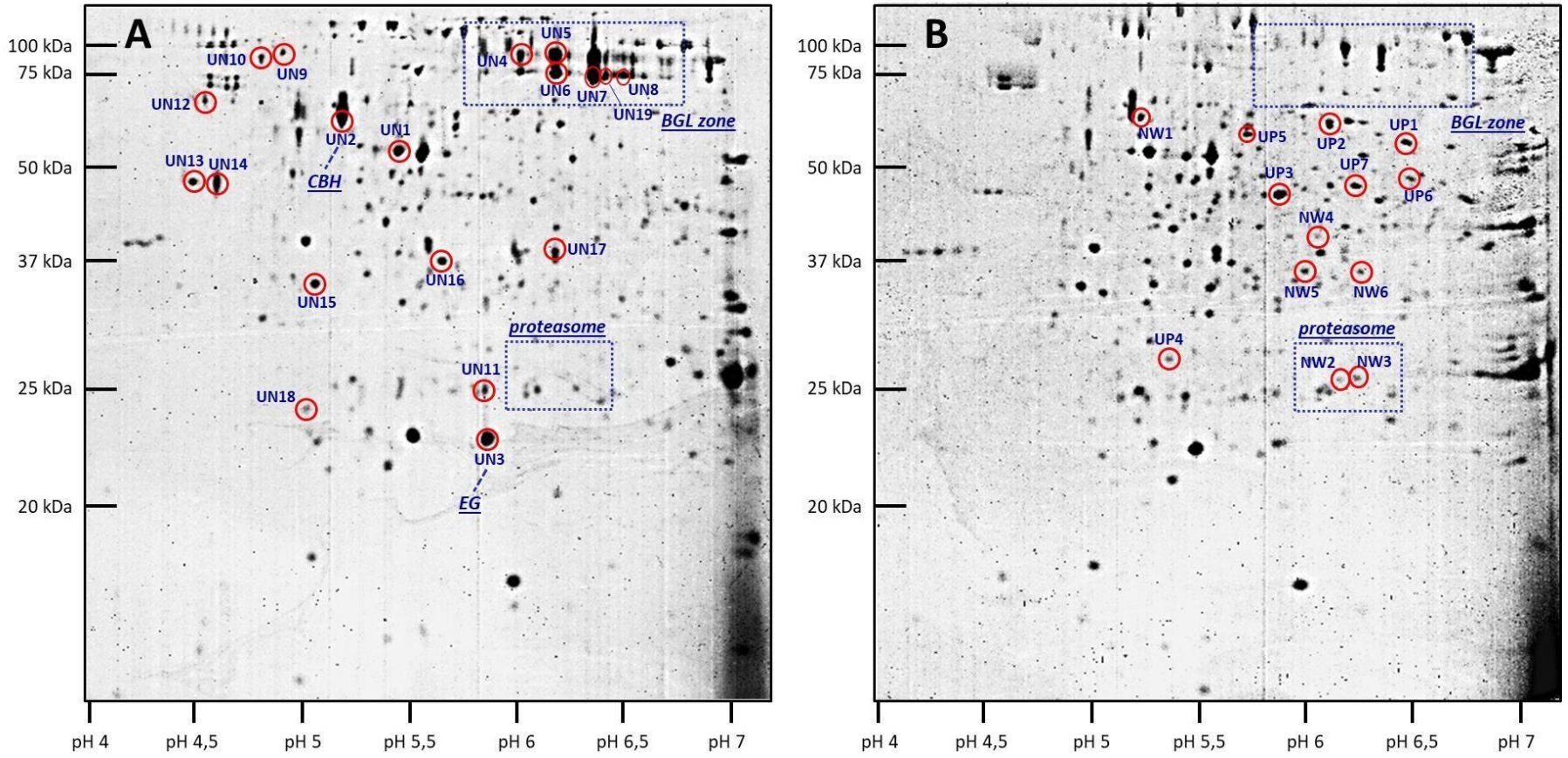

Figure 1

Click here to download high resolution image

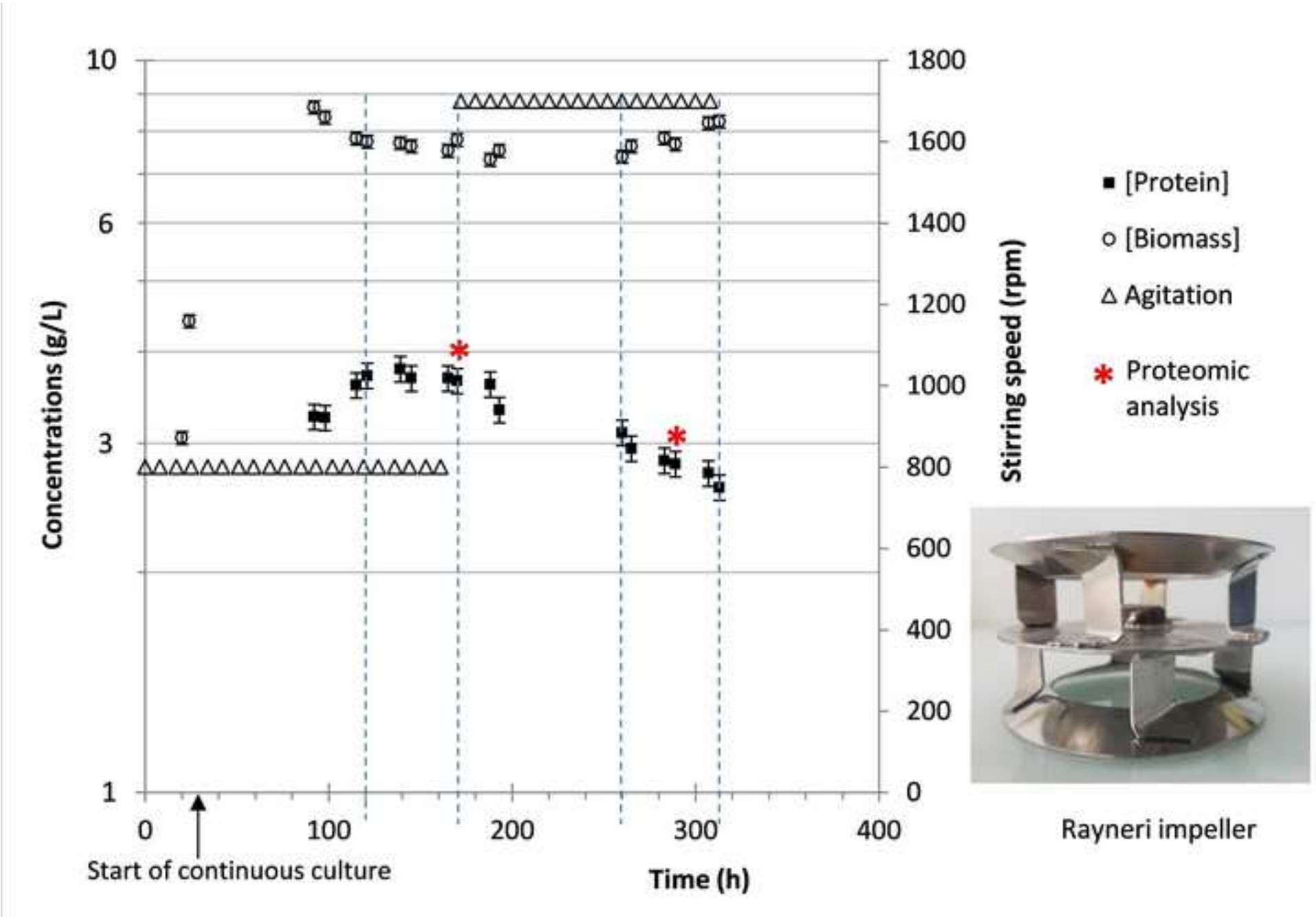

Table 1
Click here to download Table: Table 1.docx

Table 1: Measured values of culture parameters and associated p-values at the two different speeds and $EDCF_{\varepsilon max}$ values

Stirring speed	800 rpm	1700 rpm	p-value
$EDCF_{\varepsilon max}$ (kW. m^{-3}. s^{-1})	1884	38400	na
Biomass concentration, X (g. kg^{-1})	7.7 ± 0.2	7.6 ± 0.2	0.538
Specific growth rate, μ (gX. gX^{-1}. h^{-1})	0.028 ± 0.01	0.028 ± 0.03	0.064
Protein concentration, P (g. kg^{-1})	3.7 ± 0.1	2.9 ± 0.1	0.001
Specific protein (cellulases)production rate, q_p (mg. gX^{-1}. h^{-1})	13.5 ± 0.5	10.3 ± 0.8	0.0002
Specific substrate consumption rate, q_s (mg. gX^{-1}. h^{-1})	0.084 ± 0.002	0.077 ± 0.002	0.0001
β-Glucosidase activity (IU/mL)	129.0 ± 1.7	107.9 ± 1.2	0.001
$Y_{X/S}$ (g. g^{-1})	0.35 ± 0.02	0.36 ± 0.04	0.471
$Y_{P/S}$ (g. g^{-1})	0.17 ± 0.01	0.13± 0.01	0.005
$Y_{P/X}$ (g. g^{-1})	0.48 ± 0.02	0.37 ± 0.02	0.002

The data presented corresponds to the mean values for each condition (800 and 1700 rpm) for the period shown on Figure 1 and their standard deviations. Legend as in Nomenclature ; na: not applicable.

Table 2

Table 2: Proteins newly-synthesized by the increase from 800 to 1700 rpm (*EDCF*$_{\varepsilon max}$ 1884 and 38,400 kW.m^{-3}.s^{-1} respectively)

Spot	Protein ID*	Protein description	*MW* (KDa) in the 2D gel	*IP* in the 2D gel	Coverage** (%)	Functional category
NW1	135423	Chaperonin HSP60	63.1	5.25	75	Chaperone molecular family
NW2	26797	20S proteasome subunit alpha type (homologs PSMA4 / PRE9)	26.2	6.12	73	Threonine endopeptidase activity - Ubiquitin-dependent protein
NW3	99350	20S proteasome alpha type (homologs PSMA6 / SCL1)	26.3	6.30	73	
NW4	80225	Uroporphyrinogen decarboxylase	39.2	5.99	71	Porphyrin biosynthesis
NW5 & NW6***	39524	Malate dehydrogenase	35.5 35.5	5.92 6.22	37 49	Oxidoreductase activity - Carbohydrate metabolism

*MW: molecular weight; IP: isoelectric pH; *Protein ID were obtained from JGI database; **Coverage corresponds to the percentage of the protein sequence covered by identified peptides; ***Spots that correspond to isoforms of the same protein*

Table 3
Click here to download Table: Table 3.docx

Table 3: Proteins over-synthesized from the increase from 800to 1700 rpm ($EDCF_{\varepsilon max}$ 1884 and 38,400 $kW.m^{-3}.s^{-1}$ respectively)

Spot	Protein ID*	Protein description	*MW* (KDa) in the 2D gel	*IP* in the 2D gel	Coverage** (%)	Log2 fold change	Functional category
UP1	78299	Dihydrolipoyl dehydrogenase	55.3	6.47	77	1.9	Oxidoreductase activity - Cell redox homeostasis
UP2	25190	FAD/NAD(P)-binding domain-containing protein	59.5	6.07	78	1.4	
UP3	97186	Phosphomannomutase	28.1	5.38	71	1.3	GDP-mannose biosynthetic process
UP4	137356	Glutamate carboxypeptidase	57.8	5.69	82	2.5	Proteolysis
UP5	99242	Acetate kinase	46.6	6.49	81	1.3	Acetyl-CoA biosynthesis
UP6	142425	Adenosylhomocysteinase	46.0	6.22	68	1.5	Nucleic acid and amino-acid metabolism

*MW: molecular weight; IP: isoelectric pH; *Protein ID were obtained from JGI database; **Coverage corresponds to the percentage of the protein sequence covered by identified peptides*

Table 4

Click here to download Table: Table 4.docx

Table 4: Proteins under-synthesized by the increase from 800 rpm to 1700 rpm ($EDCF_{\varepsilon max}$ 1884 and 38,400 kW.m^{-3}.s^{-1} respectively)

Spot	Protein ID*	Protein description	*MW* (KDa) in the 2D gel	*IP* in the 2D gel	Coverage** (%)	Log2 fold change	Functional category
UN1	122470	Exoglucanase II (1,4-β-cellobiohydrolase)	63.5	5.22	67	-2.3	Hydrolase activity – Cellulases
UN2	124438	Endo-β -1,4-glucanase	22.8	5.81	71	-2.3	
UN3 to UN7***	136547	β-D-glucoside glucohydrolase I	94.8	5.98	66	-1.5	
			91.8	6.15	65	-1.5	
			74.9	6.15	67	-2.8	
			74.5	6.34	69	-2.6	
			75.7	6.49	71	-2.8	
UN8 & UN9***	111943	Xyloglucanase	96.5	4.97	61	-2.4	Hydrolase activity – Hemicellulase
			92.1	4.87	63	-1.5	
UN10	108605	Uracil phosphoribosyl transferase	25.4	5.82	85	-1.2	Transferase activity - Nucleoside metabolism
UN11	111063	Peptide hydrolase	67.5	4.60	58	-2.3	Proteolysis
UN12 & UN13***	102903	Putative agmatine deiminase	47.0	4.55	84	-1.5	Putrescine biosynthesis
			46.8	4.65	40	-2.6	
UN14	99640	SMP30/gluconolactonase / LRE-like protein	33.7	5.12	75	-1.2	Ca^{2+} homeostasis and signal transduction
UN15	101957	Diphosphomevalonate decarboxylase	36.0	5.63	45	-1.1	Kinase activity - ATP binding - Phosphorylation
UN16	137982	UDP-glucose 4-epimerase	37.0	6.15	39	-1.3	Coenzyme binding - Isomerase activity - Cellular metabolism
UN17	94809	NAD(P)H-dependent D-xylose reductase	24.4	5.08	53	-1.6	Oxidoreductase activity
UN18	110941	Transketolase	74.7	6.39	72	-2.9	Transferase activity – Metal ion binding - Carbohydrate metabolism

*MW: molecular weight; IP: isoelectric pH; *Protein ID were obtained from JGI database; ** Coverage corresponds to the percentage of the protein sequence covered by identified peptides; ***Spots that correspond to isoforms of the same protein*